Partial Volume Correction based on Spatial Variant Point Spread Function for Simultaneous PET-MR Imaging

Chenguang Peng[1], Jinchao Wu[1], Xingfeng Shao[1,2], Yingmao Chen[3], Quanzheng Li[4], Georges El Fakhr[4], and Kui Ying[1]

[1]Key Laboratory of Particle and Radiation Imaging, Ministry of Education, Department of Engineering, Beijing, China, [2]Department of Bioengineering, UCLA, California, United States, [3]Department of Nuclear Medicine, The general hospital of Chinese People's Liberation, Beijing, China, Beijing, China, [4]Department of Radiology, Division of Nuclear Medicine and Molecular Imaging, Harvard Medical School, Boston, United States

Target audience:

Researchers and clinicians interested in simultaneous PET-MRI imaging and Partial Volume Effect (PVE) for PET.

Purpose:

With the implementation of hybrid PET-MRI systems, simultaneously acquiring PET and MRI images becomes real. Researchers have been working on using high-resolution MRI image to improve the spatial resolution of PET image which is usually degraded by PVE [1]. Traditional Partial Volume Effect Correction (PVC) methods usually assume that the Full Width Half Maximum Height (FWHM) of the PSF is a spatial invariant constant. However, a real PET system has smaller FWHM in the center of Field of View (FOV) and larger in peripheral FOV. In our work, we proposed a method that calculated different FWHM in different regions and used MRI as prior anatomical information to enhance the spatial resolution of PET image.

Methods:

Mathematic description: In general, an acquired PET image is considered as a convolution of a real radio-activity distribution map with a Point Spread Function (PSF). The PSF is usually defined as a Gaussian function [2]. Therefore, this blurring effect could be formulated as follows:

$$I_{obs} = I_{actual} \otimes h \quad h(r) = \mathrm{A}e^{-(2.37r)^2/FWHM^2}$$

Where I_{obs} is the detected PET image and I_{actual} is real distribution, A is a scaling factor to normalize PSF, and r is the distance from the center of the h kernel.

PSF Estimation: In this work, a hybrid of frequency domain approximation and enumeration method was used to calculate the FWHM of PSF.

1. Both detected PET image and corrected image that derived from a traditional Region Based Voxel Wise (RBV) method are transformed into Fourier space. By dividing the PET frequency image by the MRI frequency image, a Fourier transform of PSF kernel is obtained. Then, a Gaussian function is fitted.
2. FWHM calculated in 1 is an approximation of real FWHM. More accurate FWHM is determined by using an enumeration method which searches for the best solution of FWHM by minimizing the following cost function.

$$argmin_{FWHM} \ \|I_{RBV} \otimes h - I_{obs}\|, \ \ h(r) = \mathrm{A}e^{-(2.37r)^2/FWHM^2}$$

Brain Phantom Simulation: A reference brain phantom was simulated by assigning tracer activity to a segmented T1-weighted MR brain image, and a cuboid cold lesion was added. The value in each tissue was assigned according to [3]. The reference distribution was divided into 6 parts based on the distance to the center of the image, which is shown in Figure 1. Each part of the reference phantom was then convolved with a particular PSF for that region. The FWHM becomes larger when the region is farther away from the center. And a simulated PET was generated by adding those convoluted regions together, which means that different region has different PVE.

Spatial Variant PSF (SVPSF) PVC method: The simulated PET image, which was generated in the last session, was divided into different regions according to different mask size (Figure.1). All regions had the same PSF FWHM 3.4 mm as the initialization. We then corrected the PSF of every region using the above-mentioned method. And Self-Adaptive (SA) PVC [4], which is recently proposed by our group, was applied for each region to generate a corrected PET image with the corrected PSF.

Results:

Figure 2 shows the comparison results of RBV and SVPSF method and their corresponding error maps. Table 1 shows the RMSE of each method in both overall region and Region of Interest (ROI) which is shown in Figure 2 with yellow square. The results indicate that proposed method performed well in both overall region and ROI. Plot 1 shows the line plots along x axis cross the center of the simulated lesion (in ROI) for each method. The low activity cubic lesion (blue square in Plot 1) has been recovered better in the proposed method. The proposed method fits the golden standard's line plot better than RBV. A clinical PET result is shown in Figure 3. The result of SVPSF demonstrates less blurring effect and better contrast.

Discussion and Conclusions:

SVPSF is proposed in this work as a MRI based PVC method to deal with the conditions where the assumption of spatially invariant PSF is not valid. Simulation results demonstrate that SVPSF outperforms RBV under a spatially variant PSF condition. The cold lesion and detailed functional activity distribution is recovered better by SVPSF than RBV. Further work could be carried out on experiments based on different PET-MRI systems.

Figure 1 Mask of reference PET division from left to right, area 1, 2, 3, 4, 5

	Area1	Area2	Area3	Area4	Area5
Real FWHM	3.4	3.8	4.2	4.6	5.0
Corrected FWHM	3.5	3.6	4.1	4.7	5.0
SVPSF RMSE	0.070	0.044	0.056	0.0543	0.089
RBV RMSE	0.228	0.302	0.255	0.255	0.268
SVPSF ROI RMSE	0.281				
RBV ROI RMSE	0.355				

Table 1 Corrected FWHM value and RMSE of RBV and SVPSF image in different area and ROI.

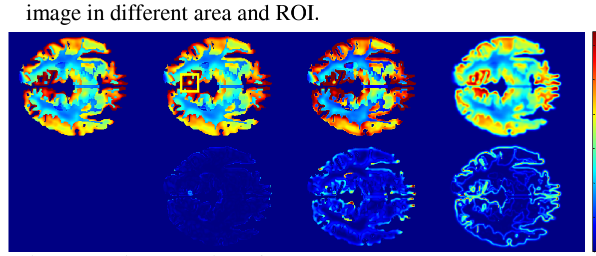

Figure 2 First row is reference, uncorrected and corrected PET images and second row is their error maps with reference PET. From left to right: Reference PET, SVPSF corrected, RBV corrected, Uncorrected. RBV is corrected with FWHM 3.4.

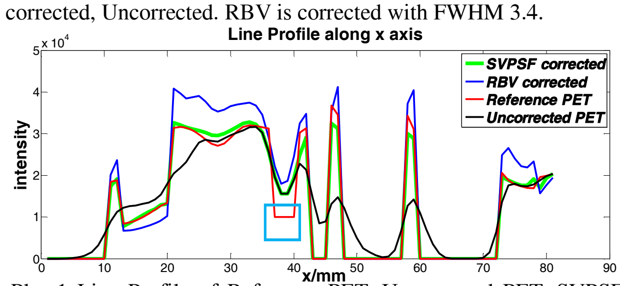

Plot 1 Line Profile of Reference PET, Uncorrected PET, SVPSF corrected PET and RBV corrected PET. Cold Lesion is in blue square.

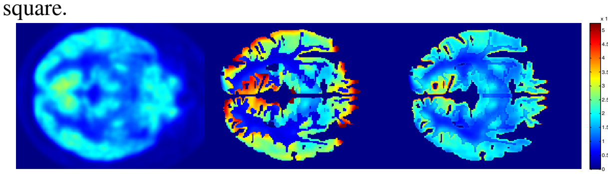

Figure 3 From left to right: Uncorrected clinical PET image, SVPSF corrected image, and RBV corrected image.

References:

[1] Kjell Erlandsson, et al. Phys. Med. Biol., 2012. [2] Yang J, et al. IEEE Transactions, 1996. [3] Muller G, et al. J Ceeb Blood Flow Metab, 1992. [4] Peng CG, et al. MIC, 2014.